

DYNAMICS OF SOME REMOTE SUPERCLUSTERS

R. J. Harms¹, H. C. Ford², and R. Ciardullo³
1. University of California, San Diego, USA
2. Space Telescope Science Institute, USA
3. University of California, Los Angeles, USA

ABSTRACT

Redshifts of clusters of galaxies have been obtained in four regions of the sky selected as suspected rich superclusters at intermediate redshift ($0.1 < z < 0.3$). Measurements to date have detected the existence of several superclusters with dimensions up to $50 h^{-1}$ Mpc ($h = H_0/100$ k/s/Mpc), irregular shapes, and containing as many as seven rich clusters in the richest supercluster. The velocity dispersions suggest some slowing of the Hubble flow internal to the superclusters. However, the inferred mass densities are low enough to prefer an open universe if the mass-to-luminosity ratios within the best-studied superclusters are comparable to the universal ratio.

1. OBSERVATIONS

Our most nearly complete redshift measurements have been obtained in the regions 1451+22 = Abell #11 (Abell 1961) = MFJG #18 (Murray et al. 1978) and 1615+43 = MFJG #19. Details of these observations are (or will be soon) published elsewhere (Ford et al. 1981, Paper I; Harms et al. 1981, Paper II; Ciardullo et al. 1983, Paper IV). Figures 1-4 summarize the locations on the sky and in redshift of the clusters of galaxies which form these two rich superclusters. Work in progress has provided less complete redshift data for several other candidate superclusters. Figures 5-8 present positions and redshifts of clusters in the directions of 0138-10 = MFJG #2 and 2306-22 = Abell #16 = MFJG #20. Note that the observations are not yet complete; candidate superclusters do contain more clusters and some may also contain additional Abell cluster members.

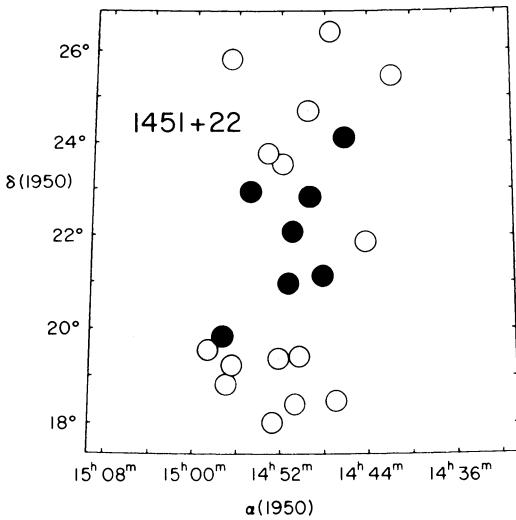


Fig. 1. Abell cluster members (filled circles) & other cluster members (open circles) of 1451+22A.

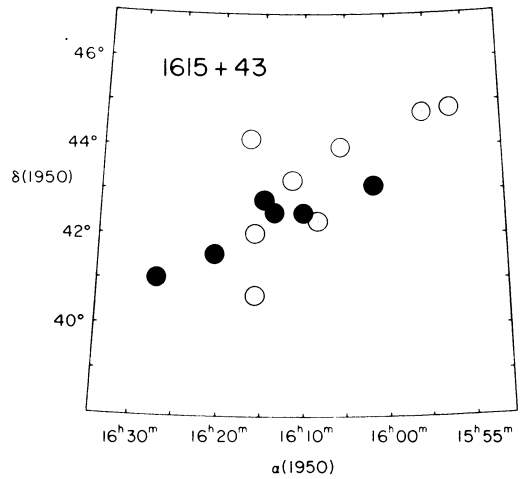


Fig. 2. Abell and other cluster members of 1615+43A.

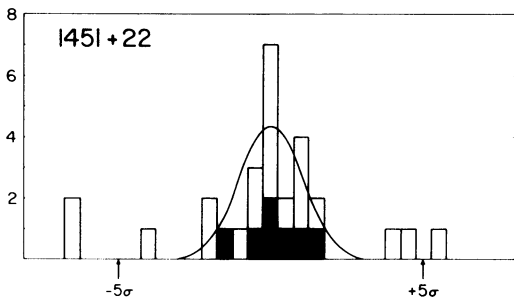


Fig. 3. No. vs redshift bin of Abell (solid) & other cluster members and near-members of 1451+22A.

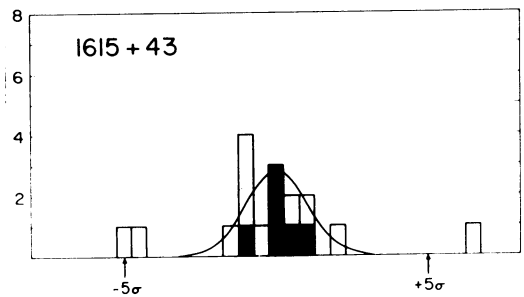


Fig. 4. No. vs redshift bin of member & near-member clusters of 1615+43A.

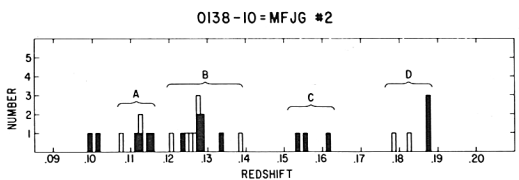


Fig. 5. Distribution of cluster redshifts toward 0138-10.

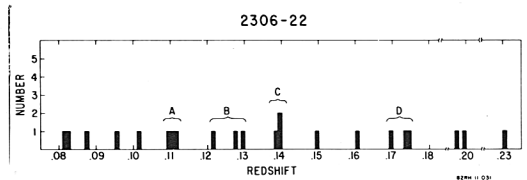


Fig. 6. Cluster (all Abell) redshifts toward 2306-22.

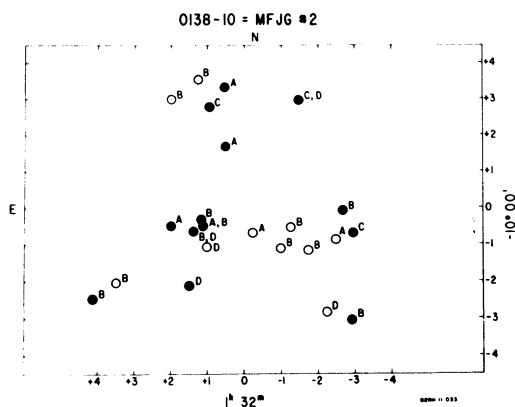


Fig. 7. Locations of clusters in 0138-10 A-D.

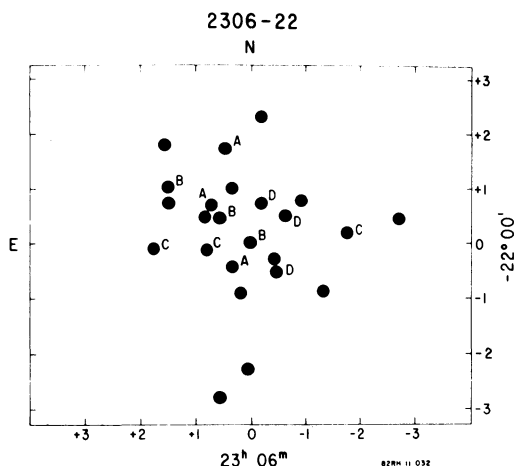


Fig. 8. Locations of Abell clusters toward 2306-22.

2. SUPERCLUSTER PROPERTIES

Table 1 lists some of the properties of the superclusters. The well-sampled superclusters 1451+22A and 1615+43A are elongated on the sky with dimensions on order of $50h^{-1}$ Mpc, while 0138-10B appears irregular but not elongated. The maps also suggest a core-halo structure in the superclusters, with Abell clusters concentrated toward the center (but often elongated) surrounded by less rich clusters. Two-color photography with crude redshift resolution capable of determining supercluster membership is underway to define the geometry and structure of the superclusters.

For both of the two well-sampled superclusters, 1451+22A and 1615+43A, the apparent thickness ΔZ (refer to Table 1) is less than the dimensions ΔX and ΔY on the sky in the α and δ directions, suggesting possible slowing of the Hubble flow within the superclusters. Table 2 summarizes the results of applying a t-test of significance to the means in ΔX , ΔY , ΔZ pairs for the four cases analyzing all or best-sampled superclusters using Abell or all cluster members. In every case, the mean ΔZ is less than the mean values for ΔX and ΔY , but always only at marginally significant levels. Two effects bias these results. We preferentially sample the full range of ΔZ but not ΔX and ΔY . Also, the measurement uncertainty in ΔZ is larger than in ΔX and ΔY due to galaxy motions in their clusters and any random cluster motions. Because both these effects lead to

TABLE 1

| Super-cluster | # Clusters | | Redshifts | | Dimensions (h^{-1} Mpc) | | | |
|---------------|------------|-------|---------------------|----------|----------------------------|------------|------------|------|
| | Abell | Total | $\langle z \rangle$ | σ | ΔX | ΔY | ΔZ | |
| 1451+22 | A | 7 | 22 | .1161 | .0019 | 24.0 | 47.4 | 21.3 |
| | B | 1 | 6 | .1019 | .0045 | 25.8 | 13.2 | 37.5 |
| | C | 2 | 4 | .1526 | .0010 | 7.2 | 42.3 | 6.3 |
| | D | 3 | 4 | .1820 | .0056 | 34.2 | 65.4 | 39.0 |
| | E | 2 | 2 | .2464 | .0049 | 6.0 | 103.2 | 20.7 |
| 1615+43 | A | 6 | 14 | .1354 | .0027 | 46.2 | 29.7 | 28.2 |
| | B | 2 | 2 | .0797 | .0001 | 15.0 | 3.3 | 0.3 |
| | C | 3 | 3 | .1845 | .0021 | 32.7 | 17.1 | 11.7 |
| 0138-10 | A | 4 | 6 | .1124 | .0028 | 26.1 | 24.6 | 24.6 |
| | B | 6 | 12 | .1275 | .0046 | 46.2 | 43.8 | 52.8 |
| | C | 3 | 3 | .1571 | .0041 | 31.8 | 30.0 | 23.7 |
| | D | 3 | 5 | .1845 | .0041 | 35.7 | 56.1 | 27.9 |
| 2306-22 | A | 3 | 3 | .1105 | .0013 | 2.4 | 12.9 | 7.5 |
| | B | 3 | 3 | .1262 | .0041 | 9.9 | 6.9 | 24.0 |
| | C | 3 | 3 | .1391 | .0007 | 24.9 | 1.8 | 3.9 |
| | D | 3 | 3 | .1725 | .0023 | 3.6 | 10.8 | 12.9 |

Supercluster properties of measured member clusters; dimensions are from extreme values of α, δ, z :

$$\Delta X = c \langle z \rangle \Delta \alpha \cos \langle |\delta| \rangle / 100h$$

$$\Delta Y = c \langle z \rangle \Delta \delta / 100h$$

$\Delta Z = c \Delta z / 100h$ with angular differences α, δ in radians

TABLE 2

| Sample Description | Sample Size | ΔX $m \pm \sigma$ | ΔY $m \pm \sigma$ | ΔZ $m \pm \sigma$ | Null Hypothesis Probability (%) | | |
|----------------------------------|-------------|------------------------------|------------------------------|------------------------------|---------------------------------|-----------------------|-----------------------|
| | | | | | $\Delta X - \Delta Y$ | $\Delta X - \Delta Z$ | $\Delta Y - \Delta Z$ |
| Best Super-clusters Abells only | 2 | 24.9 \pm 12.6 | 20.4 \pm 7.8 | 16.5 \pm 0.3 | 71 | 45 | 55 |
| Best Super-clusters all clusters | 2 | 35.1 \pm 15.6 | 38.4 \pm 12.6 | 24.6 \pm 4.8 | 84 | 46 | 29 |
| All Super-clusters Abells only* | 15 | 19.8 \pm 14.1 | 26.4 \pm 24.2 | 15.0 \pm 11.1 | 39 | 31 | 13 |
| All Super-clusters all clusters | 16 | 23.1 \pm 14.4 | 31.8 \pm 27.3 | 21.3 \pm 14.1 | 27 | 72 | 19 |

*Excluding 1451+22B, which contains only one Abell cluster

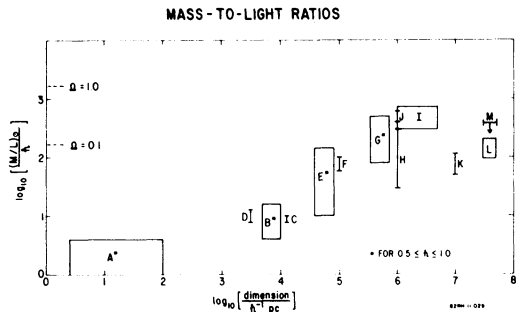
overestimating ΔZ , we conclude that the observed smallness of ΔZ probably does indicate slowing of the Hubble flow within at least some of the superclusters, but the issue is by no means resolved beyond doubt.

Neither 1451+22A nor 1615+43A show significant variation in redshift or in redshift variance with position on the sky. The less-studied 0138-10B may contain a redshift gradient in the north-south direction, but more measurements will be necessary for a reliable result.

3. COSMOLOGICAL IMPLICATIONS

The deceleration of the clusters within each supercluster is small at best. This is in qualitative agreement with the analysis in Papers I and II implying $\Omega < 0.3$ (and preferring $\Omega \approx 0.1$), assuming that the mass-to-light (or mass-to-luminous galaxy) ratios in the superclusters are typical of the universe. In any case, the seemingly inexorable increase in M/L with increasing scale appears to have halted for 1451+22A and 1615+43A, as depicted in Figure 9.

Fig. 9. Variations of M/L with scale. Samples A-K from Table 5 of Peebles (1980). L&M from Papers I and II.



REFERENCES

- Abell, G. O. 1961, *A.J.*, **66**, 607.
- Ciardullo, R., Bartko, F., Ford, H. C., and Harms, R. J. 1983, submitted to *Ap. J. Supp.* (Paper IV).
- Ford, H. C., Harms, R. J., Ciardullo, R., and Bartko, F. 1981, *Ap. J. (Letters)*, **245**, L53 (Paper I).
- Harms, R. J., Ford, H. C., Ciardullo, R., and Bartko, F. 1981, in *The Tenth Texas Symposium on Relativistic Astrophysics*, ed. R. Ramaty and F. C. Jones, (New York: New York Academy of Sciences), p. 178 (Paper II).
- Murray, S. S., Forman, W., Jones, D., and Giacconi, R. 1978, *Ap. J. (Letters)*, **219**, L89.
- Peebles, P. J. E. 1980, in *Physical Cosmology*, ed. R. Balian, J. Audouze, and D. N. Schramm, (Amsterdam, New York, Oxford: North Holland Publishing Co.), p. 213.

Discussion

Szalay: Your values of the Hubble flow seem to indicate a dynamic overdensity of 2 to 3. You mentioned a volume density contrast of 20 to 50; this would imply a highly nonlinear infall. Which is the case?

Harms: The models used were nonlinear, but easily solvable due to the simplifying approximation of spherically symmetric noncrossing mass shells for the superclusters. The initial conditions involved matching the supercluster expansion rate to the Hubble flow at "initial" redshifts ranging from 2 to 1000. The nonlinear equations for the supercluster were solved iteratively to obtain that mass within each supercluster which slows its expansion rate to the measured values at the observed epoch. Models were obtained for both the cases $\Omega \rightarrow 0$ and $\Omega = 1$; in each case the derived values for mass densities within the superclusters range from about 1 to 4 times the closure density. Note, as yet, no reference to overdensity has been made.

The luminosity contrast within the superclusters has been estimated from counts of Abell clusters, and in a preliminary fashion, from galaxy counts assuming a Schechter luminosity function. Such counts yield overdensities from about 15 to 70. If we assume these number or luminosity overdensities are similar to the mass overdensities, then we can conclude that $\Omega < 1$.